

Charge-density waves and localization in electron-irradiated $1T\text{-TaS}_2$

H. Mutka and L. Zuppiroli

Section d'Etude des Solides Irradiés, Centre d'Etudes Nucléaires, Boîte Postale n° 6, 92260 Fontenay-aux-Roses, France

P. Molinié

Laboratoire de Chimie des Solides, Centre National de la Recherche Scientifique, Université de Nantes, 2 rue de la Houssinière, 44702 Nantes, France

J. C. Bourgoin

Groupe de Physique des Solides de l'Ecole Normale Supérieure, Université de Paris 7, Tour 23, Place Jussieu, 75221 Paris, France

(Received 2 December 1980)

The relations between electronic transport, the periodic lattice distortion (PLD) associated with charge-density waves (CDW), and disorder are studied experimentally in $1T\text{-TaS}_2$. Disorder is introduced by means of electron irradiation which is able to displace lattice atoms. The effects stable around room temperature are due to displacements in the tantalum sublattice. The irradiation-induced defects act strongly on the CDW; they pin its phase and are thus able to suppress the phase transitions where the PLD orders to form a commensurate superstructure. The localized electronic ground state of the pure material can be destroyed by slight disorder to obtain metallic transport properties. Further irradiation-induced disorder leads to a new localization. This sequence is interpreted as a change from Mott to Anderson localization.

I. INTRODUCTION

A. Background

$1T\text{-TaS}_2$ is made up of covalently bound, octahedrally coordinated S-Ta-S layers which are held together by van der Waals-type forces.¹ These layers form a trigonal structure with one layer per unit cell ($1T$). This structural two-dimensionality and the strong electron-phonon coupling are the driving forces of the charge-density-wave periodic lattice distortion^{2, 3} (CDW PLD). As in other layered transition-metal dichalcogenides, transport anomalies are associated with the CDW PLD, but only in $1T\text{-TaS}_2$ a transition from a metal to a low-temperature insulator is observed.

The electrical properties of $1T\text{-TaS}_2$ have been a puzzle ever since Thompson, Gamble, and Revelli⁴ first found this metal-insulator transition. Later on the connection between the structural distortions and the electrical properties was understood in terms of the CDW PLD.^{5, 6} But it still remained a mystery why $1T\text{-TaS}_2$ shows a metal-insulator transition and not $1T\text{-TaSe}_2$, although it has a quite analogous structure. In both of these materials the low-temperature commensurate CDW creates a new two-dimensional unit cell with 13 electrons. So one does not expect to find a filled band which could give semiconducting properties (odd number of electrons), and consequently, in the case of $1T\text{-TaS}_2$, some kind of localization has to be considered.

The amount of recent experimental studies on

the electrical transport in $1T\text{-TaS}_2$ is considerable⁷⁻¹⁵ but the origin of the localization is not yet clear. Fazekas and Tosatti¹⁶⁻¹⁹ have suggested the Mott localization due to electron-electron correlation. Several authors^{7, 10, 13, 14} argue for the Anderson localization, mainly using support from the low-temperature-resistivity measurements. The importance of correlation, even in the Andersen localized state was pointed out by Fukuyama and Yosida,²⁰ who considered the large negative magnetoresistance.¹⁰ The problem seems to converge to the relative weights of charge-density waves, disorder, and correlations in determining the transport properties.

These considerations call for a study where the quantity of disorder is varied in a controlled way. This is done in the present work by introducing random defects by electron irradiation. Their effects on the electronic transport as well as on the charge-density waves are observed. The defects produced by irradiation are able to break the localization observed in the pure material and induce at higher concentration a new localized state. Comparison with substitutional disorder suggests that the irradiation drives the material from Mott to Anderson localization through a disordered metallic state.

B. Properties of $1T\text{-TaS}_2$

In $1T\text{-TaS}_2$ the CDW PLD drives two first-order phase transitions at 352 K and around 200 K. In these transitions the incommensurate CDW transforms to a commensurate superstructure.^{5, 6}

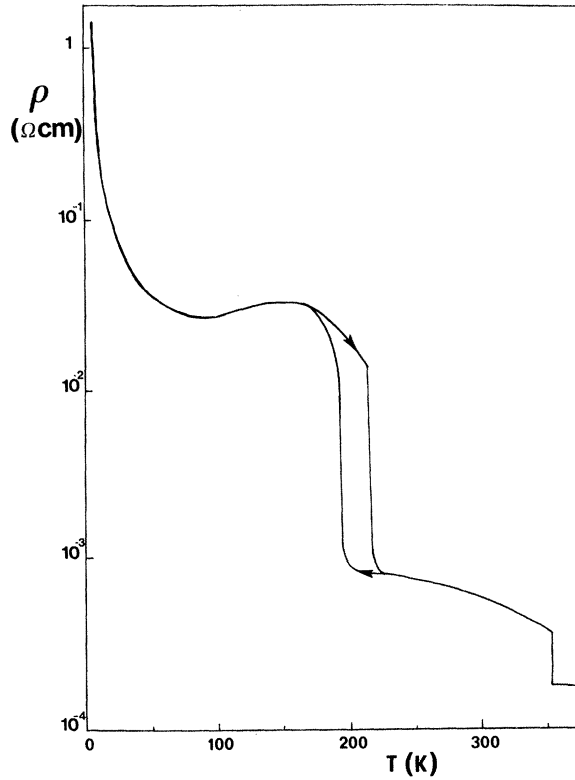


FIG. 1. The resistivity of 1T-TaS₂ as a function of temperature shows discontinuous jumps which indicate the CDW phase transitions. At low temperature a thermally activated behavior is observed.

The effects of the ordering of the CDW are clearly visible on the electronic transport. In Fig. 1, which gives the resistivity as a function of temperature, the discontinuous jumps indicate the strengthening of the CDW gapping in the electronic structure.⁵ The CDW phase transition at 200 K is also observed in the Hall effect as shown in Fig. 2.

The three distinct CDW phases correspond to different structural distortions which are visible on the electron diffraction patterns of Fig. 3. Above 352 K [Fig. 3(a)] the CDW is incommensurate; the wave vector is determined by the Fermi surface nesting.⁵ Its length depends on the filling of the conduction band as has been verified in doping²¹ and intercalation²² experiments. In the intermediate phase [Fig. 3(b)] between 200 and 352 K, the distortion is nearly commensurate with a very close-to-commensurate local order²³⁻²⁵ and, as has been proposed, with a kind of domain structure.²⁶⁻²⁸ The lock-in transition at about 200 K has a considerable hysteresis, here the CDW PLD forms a superlattice with a lattice spacing of $\sqrt{13}$ times the original [Fig. 3(c)].^{5, 6} Below 352 K the atomic displacement associated with the PLD are quite considerable, the interatomic distances

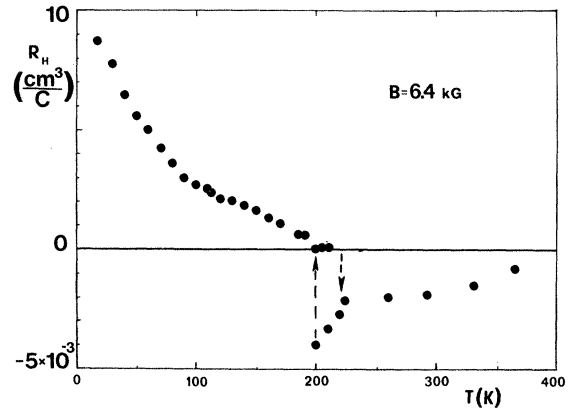


FIG. 2. The Hall coefficient obtained in a magnetic field of 6.4 kG is negative and small above 200 K. At the transition to the commensurate phase it changes sign and order or magnitude (note different scales for negative and positive values).

show variations of 15%.²⁹

As was mentioned above, the low-temperature superstructure alone cannot account for the divergence of the resistivity at low temperature (Fig. 1) and it is necessary to assume localization. Disorder can modify considerably the properties

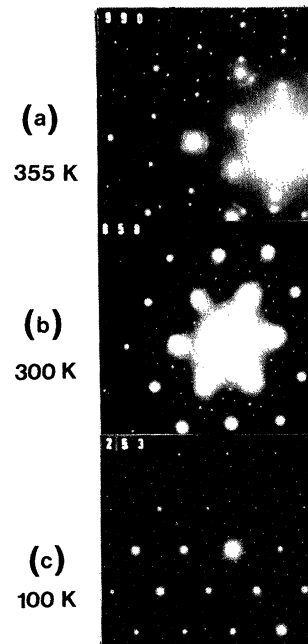


FIG. 3. Electron diffraction patterns near the basal plane (c^*) of the reciprocal lattice show the periodic lattice distortion associated to the charge-density wave. Above 352 K the distortion is incommensurate (a), around 300 K the so-called nearly commensurate one (b), and below 200 K a commensurate superstructure (c).

of $1T$ -TaS₂. About 10 at. % substitution of Ta by other transition metals causes a complete disappearance of the ordered CDW phases.^{21, 30} Disorder can enhance the existing localization¹²⁻¹⁴ or to break it and then relocalize³⁰ the conduction electrons.

In a preliminary study³¹ it was found that the CDW can be also easily perturbed by fast-neutron-irradiation-induced defects. Later, lattice parameter measurements on electron-irradiated $1T$ -TaS₂ showed a contraction in the direction perpendicular to the layers.³² This observation supports the idea that at least part of the displaced tantalum atoms go between the layers of the structure locally increasing the transverse bonding and making the material more isotropic, and it explains the strong effect of irradiation defects on the CDW.

In this paper we present results concerning the effect of electron irradiation on $1T$ -TaS₂. We have studied the defect production and we found that only the defects associated to displacement of tantalum atoms are stable at temperature above 10 K. New results on the Hall effect in disordered $1T$ -TaS₂ are reported. Electron diffraction shows that the incommensurate periodic lattice distortion is not destroyed nor does its wave vector change even at the highest defect concentration studied corresponding to 3% of displacements in the Ta sublattice.

II. EXPERIMENTAL PROCEDURES

The $1T$ -TaS₂ crystals for this study were grown by the iodine transport method at 1100 K and quenched subsequently to room temperature to retain the $1T$ structure. The dc resistivity parallel to the layers was measured by the four-points technique. The Hall effect, which is linear with the magnetic field up to 20 kG,⁸ was measured by the classical four-contact method with a magnetic field of 6.4 kG perpendicular to the layers. This was done using alternative current (33 Hz) and lock-in detection.

The electron irradiations were carried out using Van de Graaff accelerators. The resistivity curves at 21 K were obtained during irradiation in liquid H₂ at a perfectly constant temperature. The electron diffraction patterns were obtained in a Philips EM 300 electron microscope operating at 100 kV. The samples prepared by cleavage were mounted on cooling or heating holders in order to allow observations of the diffraction patterns for temperature ranging from about 100 to 400 K.

III. EXPERIMENTAL RESULTS

A. Defect production

The fast electrons (~ 1 MeV) used for irradiation lose their energy by electronic excitation and by elastic collisions with lattice atoms. Only the latter mechanism is efficient in producing permanent defects by displacing atoms.³³ When an atom is displaced far enough from its original site, a Frenkel defect is formed if the temperature is low enough to prevent migration leading to recombination or formation of complex defects.

The variation of the defect introduction rate with the energy of the bombarding electrons in $1T$ -TaS₂ has been studied in some detail. It is described elsewhere³⁴; here we present only the main results. Because of the large mass difference of the sulfur and tantalum atoms it is easy to displace them selectively. The displacement of only sulfur atoms produces qualitatively the same effects on the resistivity at 4 K as the displacement of both sulfur and tantalum atoms. However, the effects of atomic displacements in only the sulfur sublattice recover completely at temperatures around 10 K, while those obtained by displacing also tantalum partly subsist even after an anneal at 360 K.

From these observations it is concluded that the defects present after an anneal are associated with the displacements in the tantalum sublattice. Their production rate corresponds to a mean threshold energy of stable displacements of 13 ± 3 eV. Using this value and theoretical considerations^{35, 36} the number of displacements per atom (dpa) of tantalum is estimated. It provides us with a measure of disorder. High-resolution electron microscopy observation of a sample irradiated to 3×10^{-2} dpa of Ta did not show any clusters larger than 10 Å, and so the defects stable around room temperature can be very small clusters, if not point defects.

B. Effects of irradiation induced defects in $1T$ -TaS₂

The variation of resistivity with temperature for samples irradiated to different doses are shown in Fig. 4. It is readily seen that with increasing defect concentration the resistivity begins to decrease in the low-temperature region (curve 2 of Fig. 4) and the insulating phase is completely suppressed for a dose of 2×10^{-3} dpa (curve 3 of Fig. 4).

On the resistivity curves observed at 2×10^{-3} and at slightly less than 10^{-2} dpa we observe a metallic behavior at low temperature: There is clearly a finite residual resistivity with a positive slope $d\rho/dT$. Indeed, the Hall-effect results at corresponding doses (Fig. 5) confirm this obser-

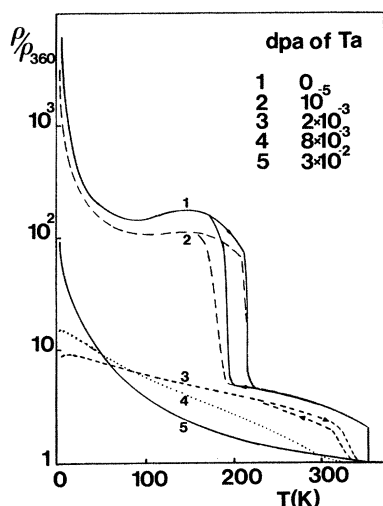


FIG. 4. Resistivity-versus-temperature curves for $1T\text{-TaS}_2$ irradiated to various doses. The thermally activated behavior of the pure and slightly disordered material is lost for a dose of 10^{-3} dpa and reappears at about 10^{-2} dpa.

vation. The low-temperature Hall coefficient that began to decrease in the beginning of the irradiation (curve 2 of Fig. 5) finally falls down to a value less than 10^{-3} times that before irradiation (curves 3 and 1 of Fig. 5). The corresponding single carrier concentration rises from 10^{18} to 10^{21} cm^{-3} . The resemblance of the Hall-coefficient curve of the disorder-induced metal (curve

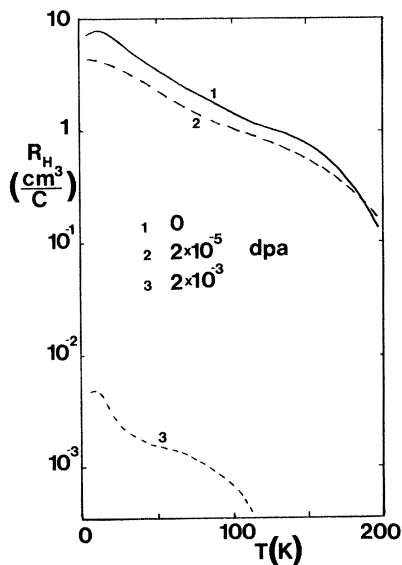


FIG. 5. Hall coefficient versus temperature for samples irradiated to various doses. Curves 1 and 2 were obtained with two samples before and after irradiation. Curve 3 is for the same sample as the resistivity curve 3 of Fig. 4.

3, Fig. 5) to that of $1T\text{-TaSe}_2$ measured by Inada, Onuki, and Tanuma¹³ is evident. Around room temperature the variation of the Hall coefficient is smaller and we always observe a negative value of the order of -5×10^{-4} cm^3/C .

But what happens to the lattice distortion which is at least partly responsible for the high value of the low-temperature resistivity before irradiation? The electron diffraction pattern obtained at 100 K [Fig. 6(a)] shows that at a dose of 8×10^{-3} dpa the commensurate distortion has given place to the nearly commensurate one normally observed down to 200 K. Consequently, this loss of commensurateness must be typical of the metallic state at low temperature.

Increasing the irradiation dose makes the transition between the incommensurate and the nearly commensurate phases less and less defined (curves 3 and 4 of Fig. 4), and finally this transition is totally suppressed from the resistivity curve (curve 5 of Fig. 4). The electron diffraction patterns obtained at the corresponding dose (3×10^{-2} dpa) show also only the incommensurate distortion down to 100 K [Figs. 6(b) and 6(c)]. It is also interesting to note that the length of the dis-

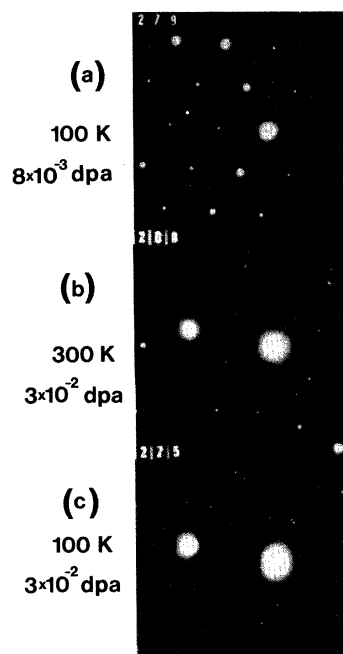


FIG. 6. The periodic lattice distortions in the irradiated samples show the suppression of the low-temperature long-range order. A sample irradiated to 8×10^{-3} dpa has the nearly commensurate distortion [compare with Fig. 3(b)] down to 100 K. At the maximum dose of 3×10^{-2} dpa the PLD is incommensurate both at 300 K (b) and at 100 K (c). Nevertheless, the length of the nesting wave vector is the same as before irradiation [compare with Fig. 3(a)].

tortion wave vector has not changed within the limits of the accuracy of the measurement. This means that the filling of the conduction band has changed less than 5%, which is already observable as shown in the alloying experiment.²¹

The low-temperature part of the resistivity curve for the most irradiated sample is worth a closer look (curve 5 of Fig. 4). The metallic residual resistivity is no longer observed, but the resistivity diverges when the temperature approaches zero. The Hall effect at this dose was measured at 295 and 140 K and in both cases, a small negative value of about 10^{-3} cm³/C was found.

Using the curve of resistivity as a function of dose (Fig. 7) we can conclude the experimental results. Even the smallest increase of disorder produced by irradiation induces a decrease of the low-temperature resistivity. After about 10^{-3} dpa, corresponding to a decrease of resistivity by a factor of 3, we observe a sudden descent of 1 order of magnitude when the long-range commensurate order is lost. We find a minimum well below the value given by the universal two-dimensional maximum metallic resistance,³⁷ at a dose corresponding to the metallic behavior in $\rho(T)$. Further irradiation increases the resistivity almost exponentially, and a continuous change to a state with thermally activated conductivity is obtained at a dose of about 10^{-2} dpa. In spite of these strong variations of the resistivity at low temperature, the room-temperature resistivity shows only an increase by a factor of 2 at a dose of 10^{-2} dpa.

IV. DISCUSSION

A. Destruction of the coherence of the CDW

We shall discuss first the ability of the irradiation induced defects to break the low-tem-

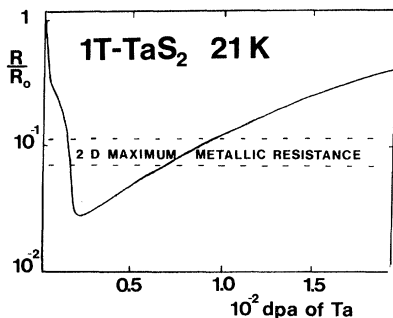


FIG. 7. Resistivity versus irradiation dose measured at 21 K during irradiation in liquid H₂. The steep descent at 10^{-3} dpa marks the loss of the commensurate CDW PLD. The resistance falls below the two-dimensional maximum metallic value (Ref. 37) and begins to increase almost exponentially with the dose.

perature ordering of the CDW without destroying the incommensurate distortion. The discussion is based on the discommensuration model of the CDW for the dichalcogenides, originally proposed by McMillan^{38,39} and later applied in detail to $1T$ -TaS₂ by Nakanishi, Shiba, Takatera, and Yamada.²⁶⁻²⁸

According to these authors the incommensurate CDW is locally very close to commensurate but full of discommensurations that are line defects of the CDW, where its phase jumps almost discontinuously. The transition to the commensurate phase is due to the disappearance of these defects of the CDW. The incommensurate CDW can be illustrated as made up of small "molecules" of varying form which locally reflect the symmetry of the commensurate CDW distortion. At the transition to the commensurate phase of $1T$ -TaS₂ all these "molecules" take the perfect star shape of 13 unit cells and long-range order is established, as described in the model of Fazekas and Tosatti.¹⁶⁻¹⁹

The screening of the perturbation due to a charged defect in a material that forms CDW's is strongly anomalous. Let us recall that in a normal metal the sharp Fermi surface creates around a point defect a damped oscillation of charge density with the period $2k_F$.⁴⁰ With the nesting Fermi surface and strong electron-phonon coupling this effect is enhanced, the defect induces a giant Friedel oscillation³ or a piece of local CDW. This effect was discussed in the layered dichalcogenides by McMillan³⁸ using the Landau free-energy model and quite recently by Tsuzuki and Sasaki^{41,42} using a self-consistent treatment in one dimension. A strong induced distortion is expected near the defect.³⁸ In the above presented local molecular picture it could be described as a "defect molecule" which has a random site in the crystal.

As a consequence, the phase of the CDW becomes pinned at the defect. Since the defects are randomly distributed, it is not possible to match the phase of the CDW between the defects; the interference creates discommensurations which stabilize the incommensurate phase toward lower temperatures. Finally, they can suppress completely the ordering of the CDW as it was observed.

This defect-induced decrease of the critical temperature of the CDW ordering is evident in Fig. 8. It gives the variation of this temperature for the incommensurate to nearly commensurate transition (originally at 352 K) as a function of disorder. The results obtained after fast neutron³¹ and electron irradiation are drawn on a single scale by normalizing the resistivity-versus-dose

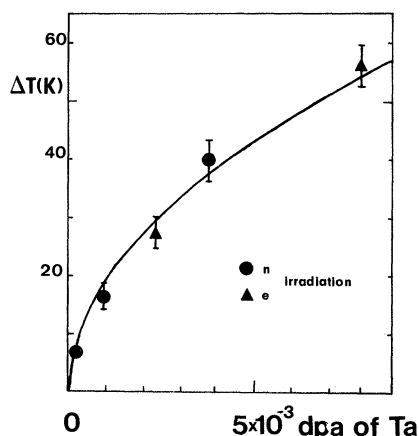


FIG. 8. Disorder decreases the critical temperature of the incommensurate to nearly commensurate transition originally at 352 K. The decrease follows the square-root dependence (full line) obtained by McMillan (Ref. 38) in the case of strongly pinning defects.

curves. The full line represents the square-root dependence on the defect concentration obtained by McMillan³⁸ in the free-energy model with strongly pinning defects. He finds also³⁸ that the defects interact by means of their CDW clouds (or giant Friedel oscillations). They tend to settle at an integer multiple of CDW wavelengths from one another, which could explain why no evidence of clustering due to the migration of the displaced atoms or of vacancies is observed.

B. From Mott to Anderson localization via a metallic state

Our experiments have demonstrated that the defects can change by several orders of magnitude the values of the resistivity and of the Hall effect at low temperatures. Meanwhile, at temperatures around 300 K, the Hall effect and the unchanged nesting wave vector show that the metallic state with the incommensurate CDW is considerably less perturbed. The latter observation is understood as follows: The thermally excited discommensurations can compensate for the mismatch between the giant Friedel oscillations due to defects. The decrease of carrier mobility due to the defect scattering explains the increase of the resistivity.

The real problems lie at low temperature: how and why the electronic states become localized or extended. We must first remember that at all concentrations of disorder there exists a periodic lattice distortion. This creates gapping in the electronic structure and the existence of localization depends on the fate of the electrons in the uppermost occupied band above the CDW condensate.

The irradiation induced disorder, even due to

the displacements in the sulfur sublattice, always has the tendency to decrease the low-temperature resistivity in the pure material. Consequently, we do not see how the Anderson localization could alone account for the diverging low-temperature resistivity.

Instead, the Mott localization model promoted by Fazekas and Tosatti¹⁵⁻¹⁹ provides a base for a coherent explanation of the observed results at low concentration of defects. Briefly, their model is the following. The narrow half filled CDW induced band which can be regarded as formed of the highest (singly) occupied molecular orbital of the 13-unit-cell star is split because of Coulomb repulsion to two Mott-Hubbard subbands.

In the discommensurations created in the commensurate CDW by irradiation-induced defects the carrier concentration is locally larger and the Mott transition is screened out. The electrons thus liberated can be more easily activated to extended states and so one observes an increase of conductivity mainly due to the increased carrier concentration (shown by our Hall-effect result (curve 2 of Fig. 1)). At the critical concentration of about 10^{-3} dpa there are more than enough defects to stabilize the nearly commensurate CDW even at low temperatures. Electron density is increased all over the crystal, there is no more Mott localization, and the electronic transport observed is metallic.

Nevertheless, it is evident that this metallic state is quite distorted, the incommensurate CDW and the giant Friedel oscillations of the defects interfere in a most incoherent way. The scattering potential of the conduction electrons is far from periodic. These effects are enhanced by further irradiation, and the diverging low-temperature resistivity reappears. What we observe is the onset of the Anderson localization when the randomness of the potential exceeds the bandwidth.⁴³ Locally seen, the material now consists mainly of the "defect molecules." Their varying shape and size induce strong modulations of electronic levels from the vicinity of one defect to the surroundings of another, and the interaction between these levels is not strong enough to create extended states.

The existence of the CDW makes the random potential as well as the conduction-electron density temperature dependent. It thus complicates the mechanism of the localization as was already noted by Di Salvo, Wilson, and Waszczak³⁰ in the case of the localization induced by doping with group-VIII B metals. Thus it is not surprising that we have not been able to fit the simple laws of the singly activated or the hopping conductivity⁴³ to our results, nor does the em-

pirical power law in T found in the case of group-VIII B doping³⁰ apply.

It is thus impossible, at least at the temperature range of our observations, to decide whether we are dealing with an activated conductivity by the extended states above the mobility edge or with a phonon-assisted hopping.⁴³ The almost exponential increase of the resistivity at 21 K with increasing disorder suggests the former behavior with a mobility edge crossing the Fermi level.

We can now compare our results to those obtained in doping experiments. The disorder induced in the tantalum sublattice by group IV B or VB substitution²¹ is considerably weaker than that due to irradiation. The effects on the CDW are similar but less pronounced as noted before.³¹ After the loss of the commensurate phase, the low-temperature resistivity can be explained reasonably by band effects^{18,19}: A maximum with clearly thermally activated behavior is observed only when the uppermost CDW induced band becomes empty. With isoelectronic doping which does not decrease the occupation in the conduction band (and is in this respect comparable to irradiation-induced defects) a strongly localized state is never observed.

The group-VIII B doping^{14,30} induces stronger disorder, which is comparable to irradiation defects. At low concentration the resistivity decreases,¹⁴ and at higher concentrations the metallic state is lost by Anderson localization.³⁰ A rapid decrease of the population of the conduction band is observed by the measurement of the length of the nesting wave vector.³⁰ Its effects probably add to those of disorder in inducing localization effects which happen at nearly the same concentration as in the case of irradiation; the effects on the CDW are anyway somewhat weaker.

The case of substitutional disorder in the sulfur sublattice¹²⁻¹⁴ is different. Its effects on the CDW PLD that is governed by the metal atom layers are subtle, and it never manages to really pin the CDW.²¹ The disorder effects it induces concern the edges of the Mott-Hubbard gap as described by Thouless⁴⁴ and discussed by Fazekas and Tosatti.^{18,19} The selenium substitution might well have a direct effect on the Coulomb correlation. It is well known that in these materials the bonding of selenium with tantalum is less ionic than with sulfur.⁴⁵ This increase of polarizability should then explain why $1T$ -TaSe₂ does not have an insulating ground state.¹⁷

In this discussion we have used the concepts of the "classical" localization theories such as the mobility edge and the two-dimensional maximum metallic resistivity. We agree with Fazekas and Tosatti^{18,19} in that they remain relevant in the case of $1T$ -TaS₂, at least from an experimental point of view. These concepts have been put in doubt by the more recent scaling theories of localization,⁴⁶ which also give new resistivity characteristics near the critical point. It is interesting to note that in the metallic state, we observe in a large interval a resistivity that decreases with increasing temperature. This is related by Imry⁴⁷ to incipient localization effects. However, in $1T$ -TaS₂ it could as well be related to the CDW effect on the free-carrier concentration.

V. CONCLUSION

The electron irradiation-induced defects are able to break the localized electronic ground state of $1T$ -TaS₂. At higher concentration they drive the material to a new, disorder-induced localization. We propose a qualitative interpretation where the effects of the defects are closely related to their strength in pinning the CDW and thus inducing local granularity in the material. The results are compared to those obtained with substitutional disorder. The irradiation-induced defects act stronger on the CDW than any substitution, as has been observed also in the organic synthetic metals.⁴⁸ Concerning the organic metals the ideas of disorder-induced granularity have been advanced by Zuppiroli *et al.*⁴⁹ Having in mind the molecular model of the commensurate CDW proposed for $1T$ -TaS₂ (Refs. 16-19) and the fact that the local order is close to commensurate in the nearly commensurate phase,²³⁻²⁵ we agree with the ideas of Fazekas and Tosatti¹⁸⁻¹⁹ of the Mott insulator as the ground state in the pure material. The correlation should also play a role in the Anderson localized state obtained by strong disorder. New information on these problems should be gained with the study of magnetic properties of the disordered $1T$ -TaS₂ which we have begun recently.

ACKNOWLEDGMENT

We thank Mrs. Nicole Housseau, who performed the high-resolution electron microscopy.

- ¹J. A. Wilson and A. D. Yoffe, *Adv. Phys.* **18**, 193 (1969).
- ²J. Friedel, in *Electron Phonon Interactions and Phase Transitions*, edited by T. Riste (Plenum, New York, 1977).
- ³R. H. Friend and D. Jerome, *J. Phys. C* **12**, 1441 (1979).
- ⁴A. H. Thompson, F. R. Gamble, and J. F. Revelli, *Solid State Commun.* **9**, 981 (1971).
- ⁵J. A. Wilson, F. J. Di Salvo, and S. Mahajan, *Adv. Phys.* **24**, 117 (1975).
- ⁶P. M. Williams, G. S. Parry, and C. B. Scruby, *Philos. Mag.* **29**, 695 (1974); **31**, 255 (1975).
- ⁷F. J. Di Salvo and J. E. Graebner, *Solid State Commun.* **23**, 825 (1977).
- ⁸R. Inada, Y. Onuki, and S. Tanuma, *Phys. Lett.* **69A**, 453 (1979).
- ⁹S. Tanuma, R. Inada, Y. Onuki, and Y. Ishizawa, *Phys. Lett.* **66A**, 416 (1978).
- ¹⁰N. Kobayashi and Y. Muto, *Solid State Commun.* **30**, 337 (1979).
- ¹¹S. Uchida, K. Tanabe, and S. Tanaka, *Solid State Commun.* **27**, 637 (1978).
- ¹²P. D. Hambourger and F. J. Di Salvo, *Physica* **99B**, 173 (1980).
- ¹³P. D. Hambourger and F. J. Di Salvo, *Solid State Commun.* **35**, 495 (1980).
- ¹⁴Y. Onuki, R. Inada, and S. Tanuma, *Physica* **99B**, 177 (1980).
- ¹⁵R. Inada, Y. Onuki, and S. Tanuma, *Physica* **99B**, 188 (1980).
- ¹⁶P. Fazekas and E. Tosatti, in *Physics of Semiconductors*, edited by F. G. Fumi (Marves-North Holland, Rome, 1976).
- ¹⁷E. Tosatti and P. Fazekas, *J. Phys. (Paris)* **37**, C4-165 (1976).
- ¹⁸P. Fazekas and E. Tosatti, *Philos. Mag. B* **39**, 229 (1979).
- ¹⁹P. Fazekas and E. Tosatti, *Physica* **99B**, 183 (1980).
- ²⁰H. Fukuyama and K. Yosida, *J. Phys. Soc. Jpn.* **46**, 1522 (1979).
- ²¹F. J. Di Salvo, J. A. Wilson, B. G. Bagley, and J. V. Waszczak, *Phys. Rev. B* **12**, 2220 (1975).
- ²²W. B. Clark and P. M. Williams, *Philos. Mag.* **35**, 583 (1977).
- ²³G. K. Wertheim, F. J. Di Salvo, and S. Chiang, *Phys. Lett.* **54A**, 304 (1975).
- ²⁴H. P. Hughes and R. A. Pollak, *Philos. Mag.* **34**, 1025 (1976).
- ²⁵T. Butz, A. Vasquez, and A. Lerf, *J. Phys. C* **12**, 4509 (1979).
- ²⁶Y. Yamada and H. Takatera, *Solid State Commun.* **21**, 41 (1977).
- ²⁷K. Nakanishi, H. Takatera, Y. Yamada, and H. Shiba, *J. Phys. Soc. Jpn.* **43**, 1509 (1977).
- ²⁸K. Nakanishi and H. Shiba, *J. Phys. Soc. Jpn.* **43**, 1839 (1977).
- ²⁹R. A. Brouwer, Ph.D. thesis, University of Groningen, Netherlands, 1978 (unpublished).
- ³⁰F. J. Di Salvo, J. A. Wilson, and J. V. Waszczak, *Phys. Rev. Lett.* **36**, 885 (1976).
- ³¹H. Mutka, D. Lesueur, and L. Zuppiroli, *Rad. Effects* **45**, 219 (1980).
- ³²H. Mutka and P. Molinie, *Solid State Commun.* **33**, 1083 (1980).
- ³³J. W. Corbett and J. C. Bourgoin, in *Points Defects in Solids*, edited by J. H. Grawford and L. M. Slifkin (Plenum, New York, 1975).
- ³⁴H. Mutka, CEA Report No. CEA-N-2170 (unpublished).
- ³⁵D. Lesueur (unpublished).
- ³⁶O. S. Oen, ORNL Reports Nos. ORNL-3813 (unpublished) and ORNL-4897 (unpublished).
- ³⁷D. C. Licciardello and D. J. Thouless, *Phys. Rev. Lett.* **35**, 1475 (1975). We attribute the maximum metallic resistance to each crystal layer of our sample. In parallel they give a resistance of the order of 10 Ω for a thickness around 100 μm .
- ³⁸W. L. McMillan, *Phys. Rev. B* **12**, 1187 (1975).
- ³⁹W. L. McMillan, *Phys. Rev. B* **14**, 1496 (1976).
- ⁴⁰J. Friedel, *Philos. Mag. Ser. 7*, **43**, 153 (1952).
- ⁴¹T. Tsuzuki and K. Sasaki, *Solid State Commun.* **33**, 1063 (1980).
- ⁴²T. Tsuzuki and K. Sasaki, *Solid State Commun.* **34**, 219 (1980).
- ⁴³N. Mott, M. Pepper, S. Pollit, R. M. Wallis, and C. J. Adkins, *Proc. R. Soc. London Ser. A* **345**, 169 (1975).
- ⁴⁴D. J. Thouless, *J. Phys. (Paris)* **37**, C4-349 (1976).
- ⁴⁵A. H. Thompson, *Phys. Rev. Lett.* **34**, 520 (1975).
- ⁴⁶See the works of E. Abrahams, P. W. Anderson, D. C. Licciardello, and T. V. Ramakrishnan, *Phys. Rev. Lett.* **39**, 1167 (1977); **42**, 673 (1979); **43**, 718 (1979), and references therein.
- ⁴⁷Y. Imry, *Phys. Rev. Lett.* **44**, 469 (1980).
- ⁴⁸G. Mihaly, L. Zuppiroli, A. Janossy, and G. Grüner, *J. Phys. C* **13**, 739 (1980).
- ⁴⁹L. Zuppiroli, S. Bouffard, K. Bechgaard, B. Hilti, and C. W. Mayer, *Phys. Rev. B* **22**, 6035 (1980).

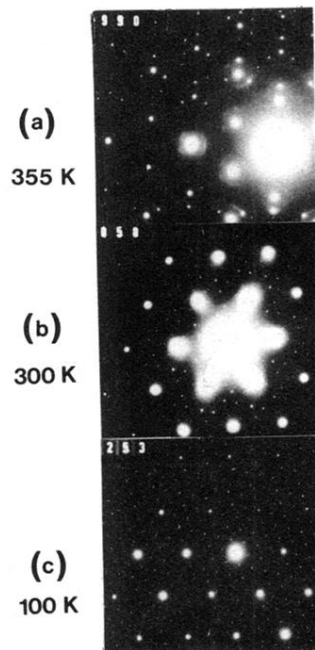


FIG. 3. Electron diffraction patterns near the basal plane (c^*) of the reciprocal lattice show the periodic lattice distortion associated to the charge-density wave. Above 352 K the distortion is incommensurate (a), around 300 K the so-called nearly commensurate one (b), and below 200 K a commensurate superstructure (c).

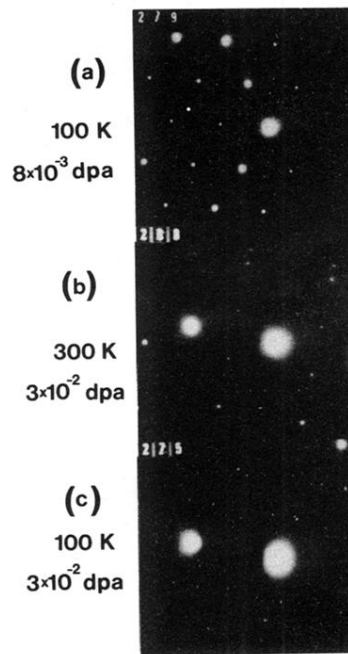


FIG. 6. The periodic lattice distortions in the irradiated samples show the suppression of the low-temperature long-range order. A sample irradiated to 8×10^{-3} dpa has the nearly commensurate distortion [compare with Fig. 3(b)] down to 100 K. At the maximum dose of 3×10^{-2} dpa the PLD is incommensurate both at 300 K (b) and at 100 K (c). Nevertheless, the length of the nesting wave vector is the same as before irradiation [compare with Fig. 3(a)].